

Augmentation of Ca_v3.2 T-type Calcium Channel Activity by cAMP-dependent Protein Kinase A

Jin-Ah Kim¹, Jin-Yong Park¹, Ho-Won Kang, Sung-Un Huh, Seong-Woo Jeong,
and Jung-Ha Lee

Department of Life Science (J.-A.K., J.-Y.P., H.-W.K., S.-U.H., J.-H.L.) and Interdisciplinary
Prorgam of Integrated Biotechnology (J.-A.K.,J.-H.L.), Sogang University, Seoul 121-742,
Korea; Department of Physiology (S.-W.J.), Institute of Basic Medical Science, Yonsei
University Wonju College of Medicine, Ilsan-Dong 162, Wonju, Korea

Running title: Augmentation of $\text{Ca}_v3.2$ Activity by PKA

The name, address, and telephone and fax numbers of the corresponding author:

Jung-Ha Lee, Ph.D

Department of Life Science, Sogang University, Mapo-Gu, Sinsu-Dong 1,

Seoul 121-742, Korea

Tel) 82-2-705-8791

Fax) 82-2-704-3126

E-mail) jhleem@sogang.ac.kr

The number of text pages: 28 pages

The number of figures: 6 figures

The number of references: 40 references

The number of words in the abstract: 217 words

The number of words in the introduction: 592 words

The number of words in the discussion: 876 words

A recommended section: Cellular and Molecular

Abbreviations: PKA, cAMP-dependent protein kinase A; LVA, low-voltage activated; HVA, high-voltage activated, 5-HT, 5-hydroxytryptamine; 5HT_7 receptor, 5-hydroxytryptamine receptor 7; H-89, *N*-[2-(*p*-bromocinnamylamino)ethyl]-5-isoquinolinesulfonamide; PKI, protein kinase A inhibitor peptide; 8-Br-cAMP, 8-bromoadenosine-3',5'-cyclic monophosphate; Rp-8-Br-cAMPS, 8-bromoadenosine-3',5'-cyclic monophosphorothioate; AKAP, PKA-anchoring protein

Abstract

Ca²⁺ influx through T-type Ca²⁺ channels is crucial for important physiological activities such as hormone secretion and neuronal excitability. However, it is not clear whether these channels are regulated by cAMP-dependent protein kinase A (PKA). In the present study, we examined whether PKA modulates Ca_v3.2 T-type channels reconstituted in *Xenopus* oocytes. Application of 10 μM forskolin, an adenylyl cyclase stimulant, increased Ca_v3.2 channel activity by 40 ± 4% over 30 min, and negatively shifted the steady state inactivation curve ($V_{50} = -61.4 \pm 0.2$ mV vs -65.5 ± 0.1 mV). Forskolin did not affect other biophysical properties of Ca_v3.2 channels including activation curve, current kinetics, and recovery from inactivation. Similar stimulation was achieved by applying 200 μM 8-Br-cAMP, a membrane permeable cAMP analog. The augmentation of Ca_v3.2 channel activity by forskolin was strongly inhibited by preincubation with 20 μM H-89, and reversed by subsequent application of 500 nM protein kinase A inhibitor peptide (PKI). The stimulation of Ca_v3.2 channel activity by PKA was mimicked by serotonin when 5HT₇ receptor was coexpressed with Ca_v3.2 in *Xenopus* oocytes. Finally, using chimeric channels constructed by replacing individual cytoplasmic loops of Ca_v3.2 with those of the Na_v1.4 channel, which is insensitive to PKA, we localized a region required for the PKA mediated augmentation to the II-III loop of the Ca_v3.2.

Introduction

Low-voltage activated (LVA) T-type Ca^{2+} channels play a key role in elevating intracellular calcium ion concentration around the resting membrane potential. Ca^{2+} influx via T-type Ca^{2+} channels regulates the pacemaker activities of sino-atrial myocytes and neuronal cells, the low-threshold calcium spikes crowned by bursting of Na^{+} -dependent action potentials in thalamic neurons, smooth muscle contraction, aldosterone and cortisol secretion in the adrenal cortex, the sperm acrosome reaction, and many types of gene expression (Hagiwara et al., 1988; Llinas and Jahnsen, 1982; Bootman et al., 2001; Pan et al., 2001; Perez-Reyes, 2003). Moreover, abnormal expression of T-type Ca^{2+} channels is involved in pathological conditions such as cardiac hypertrophy (Nuss et al., 1993; Martinez et al., 1999), epilepsy (Tsakiridou et al., 1995), and neurogenic pain (Kim et al., 2003).

To date, molecular biological studies have identified 10 genes encoding the voltage-activated calcium channel α_1 subunits that determine the primary biophysical and pharmacological properties of the channels. Expression studies have revealed that the $\text{Ca}_v3.1$ (α_{1G}), $\text{Ca}_v3.2$ (α_{1H}), and $\text{Ca}_v3.3$ (α_{1I}) genes encode low-voltage activated (LVA) T-type Ca^{2+} channel α_1 subunits, while the other genes encode high-voltage activated (HVA) Ca^{2+} channel α_1 subunits. The three T-type Ca^{2+} channels have been produced in expression systems and have been shown to possess the following biophysical and pharmacological properties: (i) activation thresholds around a resting membrane potential of -60 to -70 mV, (ii) inactivation at low voltages, (iii) slow deactivation, (iv) tiny single channel conductance, and (v) high sensitivity to kurtoxin, and mibefradil. The $\text{Ca}_v3.1$ and $\text{Ca}_v3.2$ channels generate typical T-type channel currents with transient kinetics due to fast activation and subsequent inactivation. In contrast, $\text{Ca}_v3.3$ channels produce atypical T-type channel currents with much slower kinetics.

T-type channels are primarily regulated by dynamic changes in membrane potential. Numerous studies have revealed that they are also affected by hormones and/or neurotransmitters via Ca^{2+} /calmodulin-dependent protein kinase II (Welsby et al., 2003) and protein kinase C (Park et al., 2003). Interestingly, G-protein $\beta\gamma$ subunits have shown to make a negative regulation effect on $\text{Ca}_v3.2$ T-type channel activity by interacting with the cytoplasmic loop connecting domain II and III (Wolfe et al., 2003). It has recently shown that treatment of cAMP or β -adrenergic stimulation could increase T-type channel activity in rat chromaffin cells through Epac-dependent recruitment of T-type channels (Novara et al., 2004; Giaccipoli et al., 2006).

There is controversy about whether they are regulated by cAMP-dependent protein kinase A (PKA). The majority of investigators have reported that T-type channels are little affected by PKA (Lesouhaitier et al., 2000; Pemberton et al., 2000; Lenglet et al., 2002; Bean, 1985; Benham and Tsien, 1988; Hagiwara et al., 1988; Tytgat et al., 1988; Hirano et al., 1989; Tseng et al., 1989; Fisher and Johnston, 1990). In contrast, T-type Ca^{2+} currents in frog atrial myocytes were reported to be increased by isoproterenol in two ways; a cAMP-dependent way and a cAMP-independent way (Alvarez and Vassort, 1992). In addition, Lenglet et al. (2002) also reported that T-type channel activity recorded in rat glomerulosa cells was augmented by PKA following stimulation of 5-hydroxytryptamine 7 (5HT_7) receptors.

In the present investigation, we sought to resolve the question whether T-type channel activity is regulated by PKA, using T-type $\text{Ca}_v3.2$ Ca^{2+} channels reconstituted in the *Xenopus* oocyte system. We found that $\text{Ca}_v3.2$ channel activity was significantly increased by forskolin-activated PKA. This PKA effect could be mimicked by serotonin when 5HT_7 receptor was coexpressed with $\text{Ca}_v3.2$ in *Xenopus* oocytes. In addition, we localized the region(s) of the

Ca_v3.2 channel responsible for PKA stimulation to the cytoplasmic loop connecting domains II and III.

Materials and Methods

Materials

Forskolin, H-89 {*N*-[2-(*p*-bromocinnamylamino)ethyl]-5-isoquinolinesulfonamide}, 5-HT (5-hydroxytryptamine; serotonin), 8-Br-cAMP (8-bromoadenosine-3',5'-cyclic monophosphate), Rp-8-Br-cAMPS (8-bromoadenosine-3',5'-cyclic monophosphorothioate), and protein kinase A inhibitor peptide (PKI) were purchased from Sigma (St. Louis, MO, USA). Forskolin and H-89 were diluted in DMSO to generate 10 mmol/L stock solutions. The concentration of DMSO in the bath solution is expected to be less than 0.1%, which had no effect on T-type currents. PKI, 8-Br-cAMP, and Rp-8-Br-cAMPS were prepared at stock concentrations of 1 mmol/L, 100 mmol/L and 100 mmol/L in DDW, respectively.

Construction of chimeric channels and the deletion mutant

The chimeric channels, Ca_v3.2/Na_v1.4_{N-term}, Ca_v3.2/Na_v1.4_{I-II}, Ca_v3.2/Na_v1.4_{II-III}, and Ca_v3.2/Na_v1.4_{III-IV}, were created by replacing individual cytoplasmic loops encoded by human Ca_v3.2 cDNA (α_{1H} ; GenBank accession number AF051946) with the corresponding loops of rat Na_v1.4 cDNA (μ -1; GenBank accession number NM_013178) by overlap extension PCR (Horton et al., 1989). A rat 5HT₇ receptor cDNA was obtained by RT-PCR from adrenal gland total RNA from Sprague-Dewey rats. All PCRs were performed using *Pfu* DNA polymerase (Genaxxon BioScience, Biberach, Germany). PCR products were inserted into TOPO TA cloning vector (Invitrogen, Carlsbad, CA, USA) and sequenced. Error-free PCR products were

subcloned into the original Ca_v3.2 pGEM-HEA using restriction enzyme sites (Chuang et al., 1998). Detailed information about the construction of the individual chimeric channels is given below.

Ca_v3.2/Na_v1.4_{N-term}: The N-terminus (5' polylinker - 849) of Na_v1.4 was amplified from rat Na_v1.4 cDNA using forward primer, 5'-TAATACGACTCACTATAGGG-3' (T7 primer) and reverse primer, 5'-CACGTGCTCGAACCATGGGAACAGCGCGTGAATGAG-3'. By overlap extension PCR, the amplified N-terminal cDNA was connected to the domain I portion (377 - 1227) of Ca_v3.2 amplified with forward primer, 5'-CTCATTCACGCGCTGTTCCCATGGTTCGAGCACGTG-3', and reverse primer, 5'-GATGTCGACCCAGCCTTCCAG-3', respectively. The extended cDNA was digested with *Cla*I (5'-polylinker) and *Bam*HI (729, Ca_v3.2) and ligated into Ca_v3.2 pGEM-HEA opened with *Cla*I (5'-polylinker) and *Bam*HI (729, Ca_v3.2).

Ca_v3.2/Na_v1.4_{I-II}: The cytoplasmic I-II loop (1360 - 2434) of Ca_v3.2 was replaced with the corresponding loop (1782 - 2162) of Na_v1.4. The I-II loop (1782 - 2162) of Na_v1.4 was amplified with forward primer, 5'-TTCTCGGAGACGAAGCAGGCTGAGCAGAATGAGGCT-3' and reverse primer, 5'-GTCCACGATGCGGCGCAGGTCCATGACGATCAGGTA-3'. The upstream portion (nucleotides 305-1360) preceding the Ca_v3.2 I-II loop was amplified with forward primer 5'-GCGGCCACGGTCTTCTTCTG-3' and reverse primer 5'-AGCCTCATTC TGCTCAGCCTGCTTCGTCTCCGAGAA-3'. The downstream portion (2435 - 3116) of the Ca_v3.2 I-II loop was amplified using the forward primer 5'-TACCTGATCGTCATGGACCT GCGCCGCATCGTGGAC-3' and reverse primer 5'-TGGCCACCAGCAGGTTGAAG-3'. The three PCR products were joined together by overlap extension PCR, and the extended cDNA was

digested with *NotI* and *BspEI* and ligated into Ca_v3.2 pGEM-HEA, which was opened with *NotI* (341) and *BspEI* (2637).

Ca_v3.2/Na_v1.4_{II-III}: The II-III loop (3134 - 3958) of Ca_v3.2 was replaced with the corresponding loop (2847-3518) of Na_v1.4. The II-III loop (3134 - 3958) of Na_v1.4 was amplified from Na_v1.4 cDNA using forward primer, 5'-ATCCTCGTGGAGGGCTTCAGTGCTGACAGCCTGGCG-3', and reverse primer, 5'-CACGTGATCAAACATCTTGTGCTCAACAATCTTGAA-3'. The upstream portion (2435 - 3133) preceding the Ca_v3.2 II-III loop was amplified using forward primer 5'-CGTCCGGAGCATCGTGGACAGCAA-3' and reverse primer 5'-CGCCAGGCTGTCAGCACTGAAGCCCTCCACGAGGAT-3'. The downstream portion (3938 - 4401) of the Ca_v3.2 II-III loop was amplified using forward primer 5'-TTCAAGATTGTTGAGCACAAGATGTTTGATCACGTG-3' and reverse primer 5'-AAGAAGGCGCAGCAGATGAG-3'. The II-III loop cDNA and its upstream and downstream cDNAs were joined by further PCR. The extended cDNA was digested with *BspEI* and *EcoRV*, and ligated into Ca_v3.2 pGEM-HEA that was digested with *BspEI* (2637, Ca_v3.2) and *EcoRV* (4350, Ca_v3.2).

Ca_v3.2/Na_v1.4_{III-IV}: The III-IV loop (4759 - 4915) of Ca_v3.2 was replaced with the corresponding loop (4329 - 4485) of Na_v1.4. The III-IV loop (4759 - 4915) of Na_v1.4 was amplified from rat Na_v1.4 cDNA using forward primer, 5'-GTCGAGAACTTCCACAA GCAGAAGAAGAAGTTTGGA-3' and reverse primer, 5'-ATAGTGGCTGGTGCACAGC GTCACGAAGTCGTACAC-3'. The preceding portion (3957 - 4759) of the Ca_v3.2 III-IV loop cDNA was amplified using forward primer 5'-ACAAGCTTTTTGAYCAYGTGGTCCT-3' and reverse primer 5'-TCCAAACTTCTTCTTCTGCTTGTGGAAGTTCTCGAC-3'. The following portion (4916 - 6196) of the Ca_v3.2 III-IV loop was amplified using forward primer 5'-

GTGTACGACTTCGTGACGCTGTGCACCAGCCACTAT-3' and reverse primer 5'-CTCTGCAGGATCCAGGGT-3'. The three amplified fragments were extended by additional PCR. The extended cDNA was digested with *EcoRV* and *AvrII*, and ligated into Ca_v3.2 pGEM-HEA which was opened with *EcoRV* (4350, Ca_v3.2) and *AvrII* (6170, Ca_v3.2).

Ca_v3.2_{ΔC}: Ca_v3.2_{ΔC} was constructed by deleting the carboxyl terminal portion (5774 - 6996) of Ca_v3.2. The portion (3959 - 5773) preceding the Ca_v3.2 carboxyl terminus was amplified by PCR using forward primer, 5'-ACAAGCTTTTTGAYCAYGTGGTCCT-3' and reverse primer, 5'-GGGATCCTGTCCGCGTCCA-3'. The PCR product (3959 - 5774) was digested with *SalI* and *BamHI* and ligated into Ca_v3.2 pGEM-HEA digested with *SalI* (4634) and *BamHI* (polylinker).

Cloning of rat 5HT₇ receptor cDNA

Rat adrenal gland RNA was isolated by the guanidium thiocyanate-phenol-chloroform extraction method. The first strand cDNA was synthesized from 0.5 μg of rat adrenal gland RNA with AMV reverse transcriptase (Boehringer Mannheim, Indianapolis, IN, USA) by incubation at 22°C for 10 min and then at 42°C for 50 min. The reaction was terminated by heating at 95°C for 5 min. PCR was performed using a pair of PCR primers designed based on the rat 5HT₇ receptor sequence (GenBank access numbers, NM_022938). The primer sequences were as follows: forward primer, 5'-GGCGCTCGGCACGATGATGGA-3' and reverse primer, 5'-AGCCAA TGATTTCGTTGTGTTG-3'. The PCR reaction consisted of initial denaturation at 95°C for 1 min, followed by 30 cycles of 95°C for 30 sec, 52°C for 30 sec, and 72°C for 1 min. The resulting PCR products were separated on a 1% agarose gel and purified using a gel extraction column. The purified products were ligated into TOPO TA cloning vector and transformed into

competent cells. One of three PCR products sequenced was identical to the open reading frame of NM_022938. The 5HT₇ receptor cDNA was subcloned into pGEM-HEA.

Expression of the Ca_v3.2 channel, the rat Na_v1.4 channel, their chimeric channels, and the 5HT₇ receptor in *Xenopus* oocytes

Several ovary lobes were surgically isolated from mature female *Xenopus laevis* (Xenopus Express, Haute-Loire, France) anesthetized with 0.1% of 3-aminobenzoic acid ethyl ester (Sigma, St. Louis, MO, USA). The isolated lobes were manually torn into small clusters of 5-6 oocytes in SOS solution (in mM: 100 NaCl, 2 KCl, 1.8 CaCl₂, 1 MgCl₂, 5 HEPES, 2.5 pyruvic acid, 50 µg/ml gentamicin, pH 7.6). Collagenase (Type IA, 2 mg/ml, Sigma, St. Louis, MO, USA) dissolved in Ca²⁺-free OR2 solution (in mM: 82.5 NaCl, 2.5 KCl, 1 MgCl₂, 5 HEPES, pH 7.6) was treated for about 30 minutes to remove the follicle membranes of the isolated oocytes. Stage V-VI oocytes were manually selected under a stereo-microscope and recovered in SOS solution at 18°C for several hours or overnight. Each oocyte was injected with 3-10 ng of cRNA in a volume of 40 nl using a Drummond Nanojector (Parkway, PA, USA) attached to a Narishige micromanipulator (Tokyo, Japan). All cDNAs of the T-type channel, the sodium channel, their mutant channels, and 5HT₇ receptor were linearized with *Afl*III or *Xba*I and transcribed by T7 polymerase using mMESSAGE mMACHINE T7 kits purchased from Ambion (Austin, TX, USA). For the wild type and chimeric channels (Ca_v3.2/Na_v1.4_{N-term}, Ca_v3.2/Na_v1.4_{I-II}, Ca_v3.2/Na_v1.4_{II-III} and Ca_v3.2/Na_v1.4_{III-IV}), 3-10 ng of cRNA was injected into oocytes to compare their relative expression levels. There was no significant difference between current amplitudes of the wild type and chimeric channels. In contrast, the expression level of Ca_v3.2_{ΔC} was significantly smaller than that of the Ca_v3.2 ($P < 0.01$, Student's *t* test). The

synthesized cRNA was resuspended in DEPC-treated H₂O and stored at -70°C. The 5HT₇ receptor and Ca_v3.2 channel cRNAs were injected in a molar ratio of 1 to 1.

Electrophysiological recordings and data analysis

Whole cell currents were measured with a two-microelectrode voltage clamp amplifier (OC-725C, Warner Instruments, Hamden, CT, USA) between the 3rd and 8th day after cRNA injection. Microelectrodes were pulled from capillaries (Warner Instruments, Hamden, CT, USA) and their electrode resistance was 0.2-1.0 MΩ. After the oocytes had been pricked with microelectrodes filled with 3 M KCl in SOS solution, the bath solution was exchanged with 10 mM Ba²⁺ solution (in mM: 10 Ba(OH)₂, 90 NaOH, 1 KOH, 5 HEPES, pH 7.4 with methanesulfonic acid). However, Na⁺ currents were recorded using SOS containing 100 mM NaCl. Barium currents were acquired at 5 kHz and low pass filtered at 1 kHz, and Na⁺ currents were acquired at 20 kHz and low pass filtered at 5 kHz using the pClamp system (Digidata 1320A and pClamp 8; Axon instruments, Foster City, CA, USA). Data were analyzed with Clampfit software (Axon instruments, Foster City, CA, USA) and presented graphically using Prism software (GraphPad, San Diego, CA, USA). They are presented as means ± S.E.M. and were tested for significance using Student's unpaired *t* test.

Results

Expression and characterization of human $\text{Ca}_v3.2$ T-type Ca^{2+} channels

Using the two-electrode voltage clamp method, expression of $\text{Ca}_v3.2$ (α_{1H}) channels in $\text{Ca}_v3.2$ cRNA-injected oocytes was detected as robust transient Ba^{2+} currents (> 500 nA) elicited by a test potential of -20 mV from a holding potential of -90 mV (Fig. 1A). In contrast, measurable transient Ba^{2+} currents were not detected in H_2O -injected or uninjected oocytes (data not shown). The $\text{Ca}_v3.2$ currents elicited by a voltage protocol consisting of serial test potentials increased by 10 mV from a holding potential of -90 mV displayed the typical biophysical properties of T-type channel currents, such as a low voltage threshold of about -60 mV for activation, fast activation and inactivation, criss-crossing pattern between current traces, peak current at -20 mV, and reversal potential around $+40$ mV. These properties are identical to those described in previous reports (Lee et al, 1999; Park et al., 2003).

Augmentation of $\text{Ca}_v3.2$ T-type Ca^{2+} channel activity by forskolin

When currents were evoked by a test potential to -20 mV from a holding potential of -90 mV every 20 sec, no significant run-up or run-down was observed over ≥ 30 min. (data not shown). However, application of forskolin (10 μM), an adenylyl cyclase stimulant, increased the amplitude of the $\text{Ca}_v3.2$ currents with a delay of about 2 - 3 min. The $\text{Ca}_v3.2$ current amplitude increased continuously over 30 min (Fig. 1B). Forskolin-induced stimulation of current amplitude reached a maximum level (saturation) within ~ 70 min, where they were stable or ran down slowly ($n=3$, data not shown). Representative traces before and 30 min after addition of 10 μM forskolin effect were overlapped for comparison (Fig. 1A). On average, 10 μM forskolin increased the amplitude of $\text{Ca}_v3.2$ currents by 40 ± 4 % within 30 min ($n=20$). Comparison of

current-voltage (*I-V*) relationships before and 30 min after forskolin addition showed that fold stimulations at different potentials were similar and the *I-V* curve was not shifted (Fig. 1C, D).

We also examined the effects of forskolin on other biophysical properties of the Ca_v3.2 channels including steady-state inactivation, recovery from inactivation, and current kinetics. As expected from the *I-V* relationship, the activation curves obtained from fitting cord conductance were very similar before and after forskolin treatment ($V_{50} = -34.3 \pm 0.5$ vs -34.4 ± 0.5 mV, $n=9$). In contrast, the V_{50} values of the steady-state inactivation curves before and after forskolin application were -61.4 ± 0.2 vs -65.5 ± 0.1 mV, indicating that steady state inactivation was shifted toward the negative direction (Fig. 2A; $P < 0.05$, student's *t*-test, $n=5$). Apart from the steady state inactivation, other biophysical properties such as recovery from inactivation, and the activation and inactivation kinetics of current traces, were little affected (Fig. 2B-D).

Forskolin stimulates Ca_v3.2 activity via PKA

We tested whether the forskolin effect occurs via conversion of ATP to cAMP due to stimulation of adenylyl cyclase and subsequent activation of PKA. Indeed, application of 200 μ M 8-Br-cAMP, a membrane permeable cAMP, enhanced the peak amplitude of Ca_v3.2 currents by 39 ± 8 % ($n=4$) over 30 min. The stimulation profile of 8-Br-cAMP, including delay, extent of stimulation, and time course, was very similar to that of forskolin (Fig 3). We next tested whether the forskolin effect was mediated by activation of PKA. When oocytes were preincubated in SOS containing 20 μ M H-89 {*N*-[2-(*p*-bromocinnamylamino)ethyl]-5-isoquinolinesulfonamide}, a PKA-specific inhibitor, superfusion of 10 μ M forskolin enhanced the amplitude of Ca_v3.2 currents by only 5% (Fig. 4A). Similarly, the forskolin enhancement effect was almost abolished by preincubation with 200 μ M Rp-8-Br-cAMPS, a competitive

antagonist of cAMP binding to PKA (Fig. 4B). Furthermore, the increase in the $\text{Ca}_v3.2$ current amplitude in response to forskolin could be almost completely reversed by subsequent application of 500 nM PKI, a membrane permeable PKA inhibitor peptide (Fig. 4C). Taken together, these findings indicate that the stimulation by forskolin arises from activation of the PKA signaling pathway.

Reconstitution of the PKA cascade in *Xenopus* oocytes

We coexpressed $\text{Ca}_v3.2$ channels and 5HT_7 receptors in oocytes to mimic the stimulation of PKA through a physiological second messenger system. Application of 100 nM 5-hydroxytryptamine (5-HT) increased $\text{Ca}_v3.2$ channel activity over 30 min without any tendency to saturate (Fig. 5A). Unlike the forskolin effect, the augmentation of the $\text{Ca}_v3.2$ current by 5-HT was initiated with a rapidly increasing response, without any detectable delay. The rapid uprising response was then followed by a slow increase over more than 30 min. On average, the percentage stimulation over 30 min was $60 \pm 7\%$ ($n=8$).

In oocytes pre-incubated with 20 μM H-89 followed by 5-HT, $\text{Ca}_v3.2$ current amplitude began to increase without any detectable lag, but the initial increase was not sustained; on average, the percentage augmentation of channel activity was only $16 \pm 3\%$ over 30 min (Fig. 5A), showing that 5-HT stimulation effect was strongly inhibited by H-89 pretreatment. Consistently, application of 100 nM 5-HT increased $\text{Ca}_v3.2$ peak amplitude by $57 \pm 6\%$ ($n=8$) within 30 min, and most of the 5-HT augmentation effect could be reversed by subsequent application of PKI (500 nM). A representative time course of $\text{Ca}_v3.2$ peak amplitude in response to 100 nM 5-HT, washing, and 500 nM PKI was shown in Fig. 5B. These findings demonstrate that the 5-HT stimulation effect on $\text{Ca}_v3.2$ current amplitude is mainly due to the PKA pathway.

Localization of the structural region(s) contributing to PKA-mediated stimulation

Previous studies have shown that rat Na_v1.4 is not regulated by PKA (Smith and Goldin, 1996, 2000). Accordingly, we first confirmed that rat Na_v1.4 channels expressed in oocytes were not affected by activation of PKA (Fig. 6). We then constructed chimeras of the Ca_v3.2 and Na_v1.4 channels to localize the structural regions(s) required for PKA stimulation. We constructed Ca_v3.2/Na_v1.4_{N-term}, Ca_v3.2/Na_v1.4_{I-II}, Ca_v3.2/Na_v1.4_{II-III}, and Ca_v3.2/Na_v1.4_{III-IV} by replacing individual cytoplasmic loops of Ca_v3.2 with the corresponding loops of rat Na_v1.4, and Ca_v3.2_{ΔC} was generated by truncating its carboxyl tail (Fig. 6). The expression levels of the chimeric channels were not significantly different from that of the wild type Ca_v3.2.

The activities of Ca_v3.2/Na_v1.4_{N-term}, Ca_v3.2/Na_v1.4_{I-II}, Ca_v3.2/Na_v1.4_{III-IV}, and Ca_v3.2_{ΔC} were stimulated by forskolin by $36 \pm 5\%$, $34 \pm 2\%$, $35 \pm 6\%$ and $46 \pm 8\%$, respectively, within 30 min (n=4-5). The stimulation profiles of the loop chimeras and the C-terminal truncation mutant were similar to that of wild type Ca_v3.2. In contrast, Ca_v3.2/Na_v1.4_{II-III} activity was little changed by application of forskolin (n=6; Fig. 6). On average, it was stimulated by only $2 \pm 4\%$ over 30 min, much less than observed for the wild type ($P < 0.001$, student's *t*-test). Taken together, these results strongly suggest that the II-III loop contains structural element(s) critical for the PKA stimulation.

Discussion

Electrophysiological recordings have shown that low threshold T-type currents are mainly present in adrenal glomerulosa cells (Matsunaga et al., 1987; Cohen et al., 1988; Rossier et al., 1993). *In situ* hybridization analysis has shown that of the three T-type channel isoforms, $Ca_v3.2$ is the major channel in these cells (Schrier et al., 2001). Lenglet et al. (2002) recently reported that T-type currents in rat glomerulosa were stimulated by activation of 5-HT₇ receptors via the PKA signaling pathway. These findings prompted us to test whether the channel activity of recombinant $Ca_v3.2$ reconstituted in the *Xenopus* oocyte system was regulated by PKA, and we found that channel activity was indeed enhanced by forskolin via activation of endogenous PKA.

Most previous workers have reported that T-type Ca^{2+} currents are little affected by PKA. For example, application of isoproterenol, a β -adrenergic agonist, had no effect on T-type currents recorded from either rabbit sinoatrial node (Hagiwara et al., 1988), canine atrial myocytes (Bean et al., 1985), guinea-pig ventricular myocytes (Tytgat et al., 1988), rabbit ear artery (Benham et al., 1988), canine Purkinje neuron (Hirano et al., 1989; Tseng et al., 1989), or guinea pig hippocampal CA3 neurons (Fisher and Johnston, 1990). In contrast, T-type Ca^{2+} currents recorded from frog atrial myocytes and rat glomerulosa cells were shown to be increased by the cAMP-PKA pathway (Alvarez and Vassort, 1992; Lenglet et al., 2002). The glomerulosa T-type Ca^{2+} current was increased by 5-HT via activation of the PKA signaling pathway. On the while, Alvarez and Vassort (1992) reported that T-type Ca^{2+} current in frog heart was increased by cAMP treatment and the initial cAMP-mediated increment could be further enhanced by subsequent application of isoproterenol. The cAMP-mediated response was shown to be relatively slow, while the subsequent isoproterenol response was fast. They also

displayed that the T-type Ca^{2+} current in response to isoproterenol was biphasically enhanced with fast and slow time courses. The cAMP-PKA pathway seemed to be involved in the slow response, while the mechanism (possibly G-protein mediated mechanism) responsible for the fast response remained to be uncovered. The fast and slow increment pattern of $\text{Ca}_v3.2$ channel activity by 5-HT shown in this study was somewhat similar to the isoproterenol regulation pattern of frog T-type Ca^{2+} current. It is also similar to the case of the isoproterenol regulation of frog T-type channel current that the up-regulation of $\text{Ca}_v3.2$ current activity in response to forskolin or 5-HT was obtained from oocytes of 11 frogs out of 15 frogs. On the contrary, $\text{Ca}_v3.2$ T-type channel currents of oocytes isolated from the other 4 frogs did not show any enhancement to those drugs. Taken together, these different regulation results suggest that the PKA regulation effects on T-type channel currents can be variable between tissues expressing T-type channels.

Native L-type Ca^{2+} currents recorded in cardiac myocytes were strongly upregulated by PKA, whereas recombinant cardiac L-type Ca^{2+} channel currents recorded in HEK293 cells were essentially unaffected (Mikala et al., 1998; Zong et al., 1995). This discrepancy was resolved by the finding that stimulation of cardiac L-type channel currents depended on the presence or absence of AKAP (a PKA-anchoring protein) which played a crucial role in localizing PKA near to the plasma membrane (Fraser et al., 1998; Gao et al., 1997). However, AKAP is not likely to be a critical factor affecting the regulation of T-type channel activity, because T-type currents are insensitive to PKA in cardiac myocytes, in which AKAP is expressed (Gray et al., 1998). The different effects on T-type channels may depend on the presence or absence of unidentified proteins that prevent PKA from interacting with the channels. A related possibility is that T-type currents are up-regulated by activation of PKA via phosphorylation of an accessory subunit rather than the $\text{Ca}_v3.2$ α_1 subunit itself, as shown for $\text{K}_v1.5$ whose regulation by PKA is reported

to be via phosphorylation of $K_v\beta 1.3$ (Kwak et al., 1999). Therefore, further efforts should be made to identify regulatory proteins or auxiliary subunits of the T-type channel α_1 subunit.

We localized a structural region contributing to the augmentation of $Ca_v3.2$ activity to the II-III loop of the $Ca_v3.2$. To identify a specific locus for phosphorylation by PKA in the II-III loop, we tested the role of Thr1055, Ser1133, and Ser1134 by making point mutation converting them individually into Ala because these sites are found in the motifs (Arg-Arg-X-Ser/Thr or Arg-X(X)-Ser/Thr) known to be phosphorylated by PKA, and are conserved in the three T-type channel isoforms. All of the mutant channels were regulated by forskolin and their regulatory profiles were similar to that of wild type $Ca_v3.2$, suggesting that these sites do not contribute to the PKA-mediated stimulation. In addition to the three sites examined, there are 8 more putative sites fitting the consensus motifs for PKA phosphorylation. Their involvement(s) remains to be investigated by making individual point mutations.

In summary, we have shown that $Ca_v3.2$ channel activity can be up-regulated by PKA and we were able to reconstitute the PKA signaling pathway augmenting T-type channel activity in *Xenopus* oocytes. In addition, we localized the structural region involved in the PKA stimulation to the II-III loop. The PKA stimulation of cloned T-types Ca^{2+} channels in the *Xenopus* oocyte system demonstrated here may contribute to understanding T-type channel regulation by neurotransmitters and hormones.

Acknowledgement

Jin-Ah Kim and Jin-Yong Park contributed equally to this work.

References

- Alvarez JL and Vassort G (1992) Properties of the low threshold Ca current in single frog atrial cardiomyocytes. *J Gen Physiol* **100**:519-545.
- Bean BP (1985) Two kinds of calcium channels in canine atrial cells; Differences in kinetics, selectivity, and pharmacology. *J Gen Physiol* **86**:1-30.
- Benham CD and Tsien RW (1988) Noradrenaline modulation of calcium channels in single smooth muscle cells from rabbit ear artery. *J Physiol* **404**:767-784.
- Bootman MD, Collins TJ, Peppatt CM, Prothero LS, Mackenzie L, Desmet P, Travers M, Tovey SC, Seo JT, Berridge MJ, Ciccolini F and Lipp P (2001) Calcium signaling-an overview. *Semin Cell Dev Biol* **12**:3-10.
- Chuang RS, Jaffe H, Cribbs L, Perez-Reyes E and Swartz KJ (1998) Inhibition of T-type voltage-gated calcium channels by a new scorpion toxin. *Nat Neurosci* **1**:668-674.
- Cohen CJ, McCarthy RT, Barrett PQ and Rasmussen H (1988) Ca channels in adrenal glomerulosa cells: K⁺ and angiotensin II increase T-type Ca channel current. *Proc Natl Acad Sci USA* **85**:2412-2416.
- Fisher R and Johnston D (1990) Differential modulation of single voltage-gated calcium channels by cholinergic and adrenergic agonists in adult hippocampal neurons. *J Neurophysiol* **64**:1291-1302.
- Fraser ID, Tavalin SJ, Lester LB, Langeberg LK, Westphal AM, Dean RA, Marrion NV and Scott JD (1998) A novel lipid-anchored A-kinase anchoring protein facilitates cAMP-responsive membrane events. *EMBO J* **17**:2261-2272.

- Gao T, Yatani A, Dell'Acqua ML, Sako H, Green SA, Dascal N, Scott JD and Hosey MM (1997) cAMP-dependent regulation of cardiac L-type Ca^{2+} channels requires membrane targeting of PKA and phosphorylation of channel subunits. *Neuron* **19**:185-196.
- Giancippoli A, Novara M, de Luca A, Baldelli M, Marcantoni A, Carbone E and Carabelli V (2006) Low-threshold exocytosis induced by cAMP-recruited $\text{Ca}_v3.2$ (α_{1H}) channels in rat chromaffin cells. *Biophys J* **90**:1830-1841.
- Gray PC, Johnson BD, Westenbroek RE, Hays LG, Yates III JR, Scheuer T, Catterall WA and Murphy BJ (1998) Primary structure and function of an A kinase anchoring protein associated with calcium channels. *Neuron* **20**:1017-1026.
- Hagiwara N, Irisawa H and Kameyama M (1988) Contribution of two types of calcium currents to the pacemaker potentials of rabbit sino-atrial node cells. *J Physiol* **395**:233-253.
- Hirano Y, Fozzard HA and January CT (1989) Inactivation properties of T-type calcium current in canine cardiac Purkinje cells. *Biophys J* **56**:1007-1016.
- Horton RM, Hunt HD, Ho SN, Pullen JK and Pease LR (1989) Engineering hybrid genes without the use of restriction enzymes: gene splicing by overlap extension. *Gene* **77**:61-68.
- Kameyama M (1988) Contribution of two types of calcium currents to the pacemaker potentials of rabbit sino-atrial node cells. *J Physiol* **395**:233-253.
- Kim D, Park D, Choi S, Lee S, Sun M, Kim C and Shin H (2003) Thalamic control of visceral nociception mediated by T-type Ca^{2+} channels. *Science* **302**:117-119.
- Kwak YG, Hu N, Wei J, George ALJ, Grobaski TD, Tamkun MM and Murray KT (1999) Protein kinase A phosphorylation alters $\text{K}_v\beta 1.3$ subunit-mediated inactivation of the $\text{K}_v1.5$ potassium channel. *J Biol Chem* **274**:13928-13932.

Lee J-H, Daud AN, Cribbs LL, Lacerda AE, Pereverzev A, Klockner U, Schneider T and Perez-Reyes E (1999) Cloning and expression of a novel member of the low voltage-activated T-type calcium channel family. *J Neurosci* **19**:1912-1921.

Lenglet S, Louiset E, Delarue C, Vaudry H and Contesses V (2002) Activation of 5-HT₇ receptor in rat glomerulosa cells is associated with an increase in adenylyl cyclase activity and calcium influx through T-type calcium channels. *Endocrinology* **143**:1748-1760.

Lesouhaitier O, Kodjo MK, Cartier F, Contesses V, Yon L, Delarue C and Vaudry H (2000) The effect of the endozepine triakontatetraneuropeptide on corticosteroid secretion by the frog adrenal gland is mediated by activation of adenylyl cyclase and calcium influx through T-type calcium channels. *Endocrinology* **141**:197-207.

Llinas R and Jahnsen H (1982) Electrophysiology of mammalian thalamic neurons in vitro. *Nature* **297**:406-408.

Martinez ML, Heredia MP and Delgado C (1999) Expression of T-type Ca²⁺ channels in ventricular cells from hypertrophied rat hearts. *J Mol Cell Cardiol* **31**:1617-1625.

Matsunaga H, Yamashita N, Maruyama Y, Kojima I and Kurokawa K (1987) Evidence for two distinct voltage-gated calcium channel currents in bovine adrenal glomerulosa cells. *Biochem Biophys Res Commun* **149**:1049-1054.

Mikala G, Klockner U, Varadi M, Eisfeld J, Schwartz A and Varadi G (1998) cAMP-dependent phosphorylation sites and macroscopic activity of recombinant cardiac L-type calcium channels. *Mol Cell Biochem* **185**:95-109.

Novara M, Baldelli P, Cavallari D, Carabelli V, Giaccipoli A and Carbone E (2004) Exposure to cAMP and β -adrenergic stimulation recruits Ca_v3 T-type channels in rat chromaffin cells through Epac cAMP-receptor proteins. *J Physiol* **558**:433-449.

- Nuss HB and Houser SR (1993) T-type Ca^{2+} current is expressed in hypertrophied adult feline left ventricular myocytes. *Circ Res* **73**:777-782.
- Pan ZH, Hu HJ, Perring P and Andrade R (2001) T-type Ca^{2+} channels mediate neurotransmitter release in retinal bipolar cells. *Neuron* **32**:89-98.
- Park J-Y, Jeong S-W, Perez-Reyes E and Lee J-H (2003) Modulation of $\text{Ca}_v3.2$ T-type channels by protein kinase C. *FEBS Lett* **547**:37-42.
- Pemberton KE, Hill-Eubanks LJ and Jones SV (2000) Modulation of low-threshold T-type calcium channels by the five muscarinic receptor subtypes in NIH 3T3 cells. *Pflügers Arch* **440**:452-461.
- Perez-Reyes E (2003) Molecular physiology of low-voltage activated T-type calcium channels. *Physiol Rev* **83**:117-161.
- Rossier MF, Python CP, Capponi AM, Schlegel W, Kwan CY and Vallotton MB (1993) Blocking T-type calcium channels with tetrandrine inhibits steroidogenesis in bovine adrenal glomerulosa cells. *Endocrinology* **132**:1035-1043.
- Schrier AD, Wang H, Talley EM, Perez-Reyes E and Barrett PQ (2001) α_{1H} T-type Ca^{2+} channel is the predominant subtype expressed in bovine and rat zona glomerulosa. *Am J Physiol* **280**:C265-272.
- Smith RD and Goldin AL (1996) Phosphorylation of brain sodium channels in the I-II linker modulates channel function in *Xenopus* oocytes. *J Neurosci* **16**:1965-1974.
- Smith RD and Goldin AL (2000) Potentiation of rat brain sodium channel currents by PKA in *Xenopus* oocytes involves the I-II linker. *Am J Physiol* **278**:C638-645.

- Tsakiridou E, Bertollini L, de Curtis M, Avanzini G and Pape HC (1995) Selective increase in T-type calcium conductance of reticular thalamic neurons on a rat model of absence epilepsy. *J Neurosci* **15**:3110-3117.
- Tseng GN and Boyden PA (1989) Multiple types of Ca^{2+} currents in single canine Purkinje cells. *Circ Res* **65**:1735-1750.
- Tytgat J, Nilius B, Vereecke J and Carmeliet E (1988) The T-type Ca^{2+} channel in guinea-pig ventricular myocytes is insensitive to isoproterenol. *Pflügers Arch* **411**:704-706.
- Welsby PJ, Wang H, Wolfe JT, Colbran RJ, Johnson ML and Barrett PQ (2003) A mechanism for the direct regulation of T-type calcium channels by Ca^{2+} /calmodulin-dependent kinase II. *J Neurosci* **23**:10116-10121.
- Wolfe JT, Wang H, Howard J, Garrison JC and Barrett PQ (2003) T-type calcium channel regulation by specific G-protein $\beta\gamma$ subunits. *Nature* **424**:209-213.
- Zong X, Schreieck J, Mehrke G, Welling A, Schuster A, Bosse E, Flockerzi V and Hofmann F (1995) On the regulation of the expressed L-type calcium channel by cAMP-dependent phosphorylation. *Pflügers Arch* **430**:340-347.

Footnotes

Financial support: This work was supported by the Korea Research Foundation Grants funded by the Korean government (KRF-2005-015-C00403 and KRF-2005-042-C00058).

Figure Legends

Figure 1. Effect of 10 μ M forskolin on human $\text{Ca}_v3.2$ T-type channel

(A) Representative current traces before (a) and 30 min after forskolin application (b) are overlapped. (B) Time course of forskolin-mediated stimulation of $\text{Ca}_v3.2$ channel activity. A representative time course is plotted. The $\text{Ca}_v3.2$ current was evoked by a test potential of -20 mV from a holding potential of -90 mV every 20 sec, using 10 mM Ba^{2+} as charge carrier. Current amplitude was normalized to the control current amplitude before forskolin application. $\text{Ca}_v3.2$ activity was increased by $40 \pm 4\%$ in response to 10 μ M forskolin within 30 min ($n=20$). (C) Current-voltage relationship. Currents were evoked by depolarizing voltage steps in 10 mV increments from -70 to +40 mV from a holding potential of -90 mV. Peak currents obtained during test potentials were normalized to the maximum observed. (D) Peak currents were normalized to the maximum observed before the application of forskolin (control, ●; forskolin application, ○).

Figure 2. Biophysical properties of human $\text{Ca}_v3.2$ T-type channels before and after forskolin treatment

(A) Steady-state activation and inactivation curves before (●) and 30 min after (○) application of forskolin. Activation curves were obtained by plotting chord conductances (G), which were calculated by dividing the current amplitude by the driving force. Smooth curves represent the fit of the data to the Boltzman equation ($G = 1 / [1 + \exp(V_{50} - V)/k]$), where V_{50} is the half-activation voltage, and k is a slope factor. (B) Time course of recovery from inactivation before and 30 min after forskolin application. Data are averaged and fitted by single exponential association. (C) and (D) The activation and inactivation taus (τ) of the current traces were obtained by fitting

them with two exponentials simultaneously, one for the activation kinetics and the other for the inactivation kinetics.

Figure 3. 8-Br-cAMP mimics the forskolin effect on human Ca_v3.2 T-type channels

(A) Representative time course of the effect of 200 μ M 8-Br-cAMP on the peak current amplitude of Ca_v3.2. Currents were evoked by a test potential of -20 mV from a holding potential of -90 mV every 20 sec and their amplitudes were normalized to the control current amplitude before 8-Br-cAMP treatment. Ca_v3.2 channel activity increased by $39 \pm 8\%$ (n=4) over 30 min in response to 200 μ M 8-Br-cAMP (B) Representative current traces before (a) and 30 min after 8-Br-cAMP application (b) are overlapped.

Figure 4. Attenuation of the forskolin effect on Ca_v3.2 channel activity by H-89, Rp-8-Br-cAMPS, and PKI

(A) Average time courses of the effect of 10 μ M forskolin on peak current amplitude of Ca_v3.2 in the absence (control) and presence of 20 μ M H-89. Preincubation with 20 μ M H-89 strongly attenuated forskolin stimulation. The percentage stimulation of Ca_v3.2 activity by 10 μ M forskolin was $40 \pm 4\%$ over 30 min (control, \circ , n=20). In contrast, preincubation with 20 μ M H-89 reduced stimulation to $5 \pm 3\%$ (\square , n=4). (B) Average time courses of peak current amplitude of Ca_v3.2. Preincubation with 200 μ M Rp-8-Br-cAMPS abolished the forskolin stimulation effect (n=4). (C) Reversal of the forskolin augmentation effect by PKI. Application of 10 μ M forskolin enhanced Ca_v3.2 peak amplitude by $36 \pm 4\%$ (n=4) within 30 min. The forskolin effect was almost reversed by subsequent application of PKI (500 nM). A representative time course of

Ca_v3.2 current amplitude in response to forskolin and washing followed by addition of PKI is plotted.

Figure 5. Stimulation of 5HT₇ receptors augments Ca_v3.2 channel activity via PKA

(A) The effect of 5-HT stimulation of Ca_v3.2 channel activity with or without preincubation with 20 μ M H-89 is plotted against time. Ca_v3.2 channel activity was recorded in oocytes co-injected with Ca_v3.2 channel and 5HT₇ receptor cRNAs. The voltage protocol was the same as that described in Fig.1. Stimulation of the 5HT₇ receptor with 100 nM 5-HT enhanced Ca_v3.2 activity by $60 \pm 7\%$ over 30 min (\circ , n=8) and stimulation was significantly reduced to $16 \pm 3\%$ by preincubation with 20 μ M H-89 (\square , n=4). (B) Reversal of the 5-HT stimulation effect by PKI. A representative time course of Ca_v3.2 current amplitude in response to 100 nM 5-HT and washing followed by addition of PKI is plotted (n=8).

Figure 6. Comparison of forskolin effects on Ca_v3.2, Na_v1.4, and their mutant channels

Schematic diagrams of Ca_v3.2, its deletion mutant, the loop chimeras, and Na_v1.4 are shown on the left. Ca_v3.2 is illustrated by white cylinders and thin lines, and Na_v1.4 by gray cylinders and thick lines. Accordingly, the thick lines of the chimeric channels are derived from Na_v1.4. Changes of peak current amplitudes caused by 10 μ M forskolin were evaluated within 30 min and average stimulation percentages are plotted as bar graphs on the right (mean \pm SEM, n=4-6). Significant differences were evaluated using the *t*-test, and differences with $P \leq 0.001$ are designated by ***. The numbers of oocytes tested are given in parentheses.

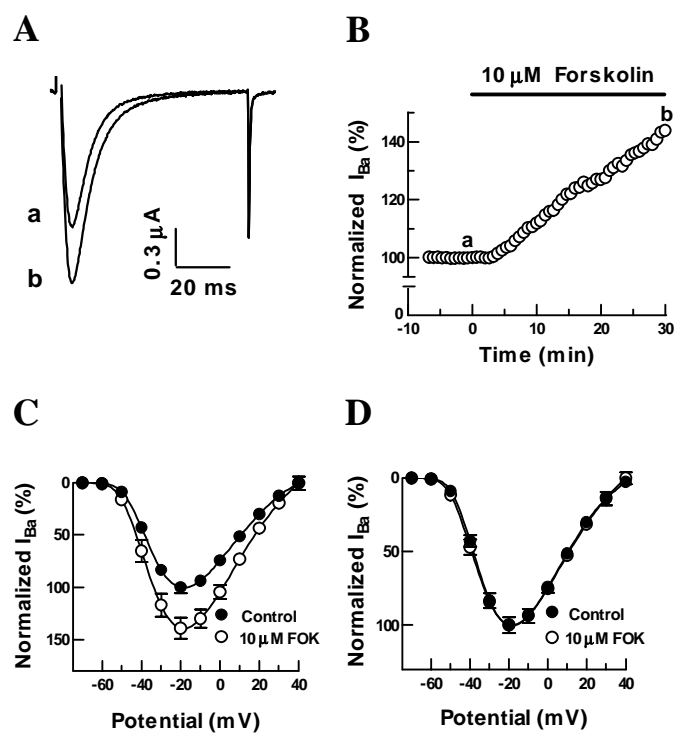


Figure 1

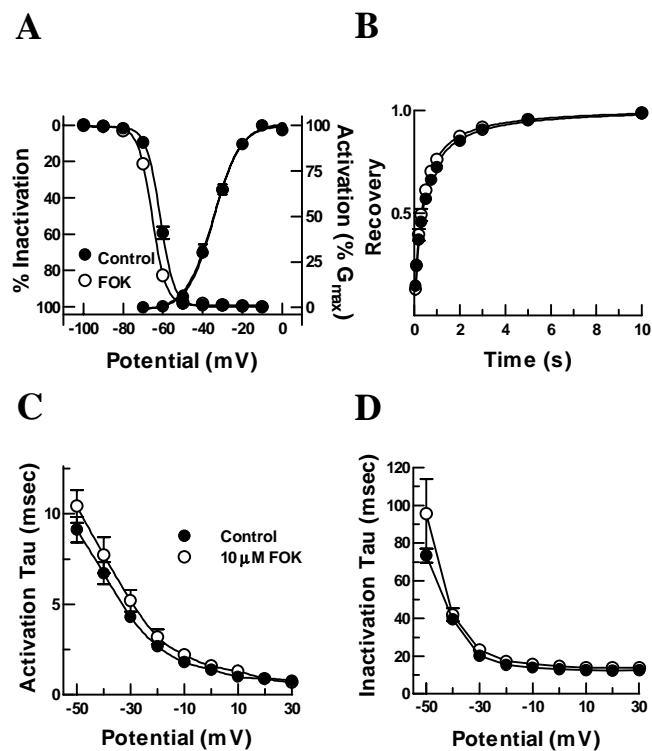


Figure 2

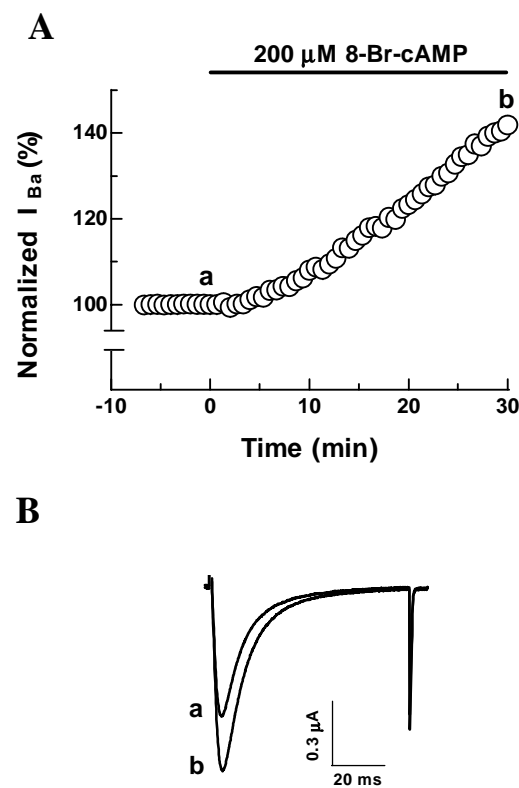


Figure 3

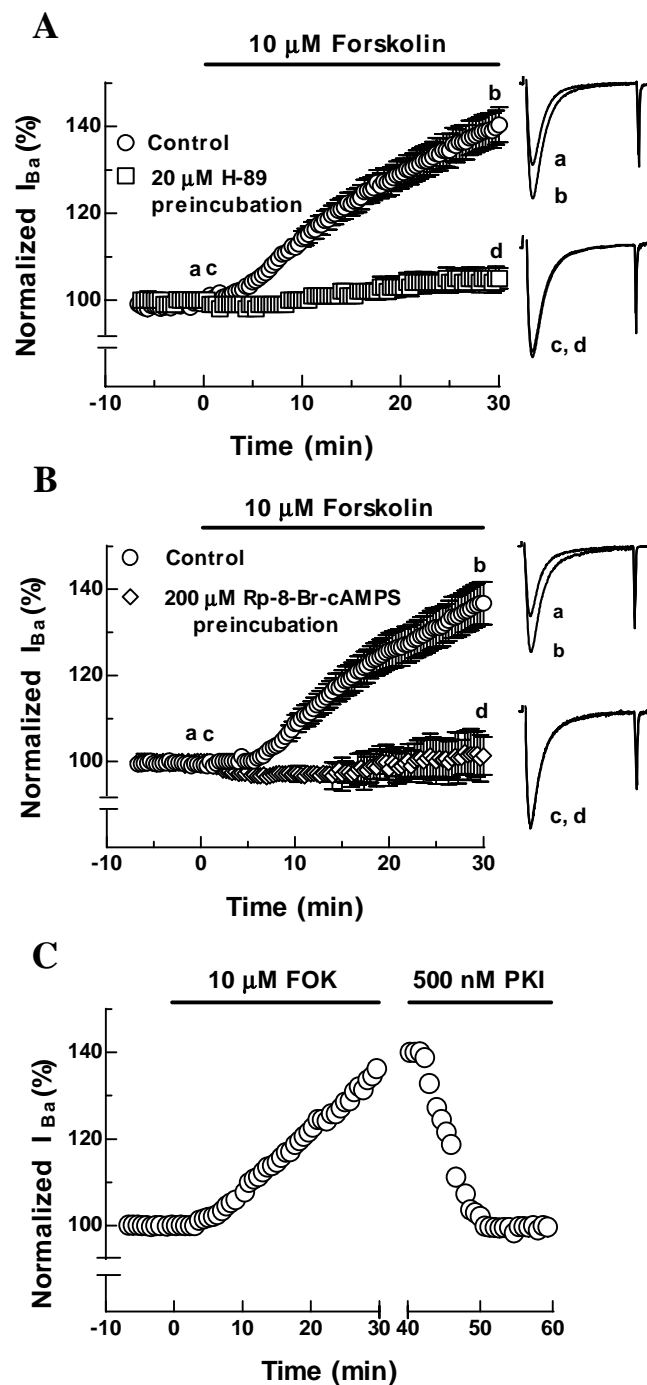


Figure 4

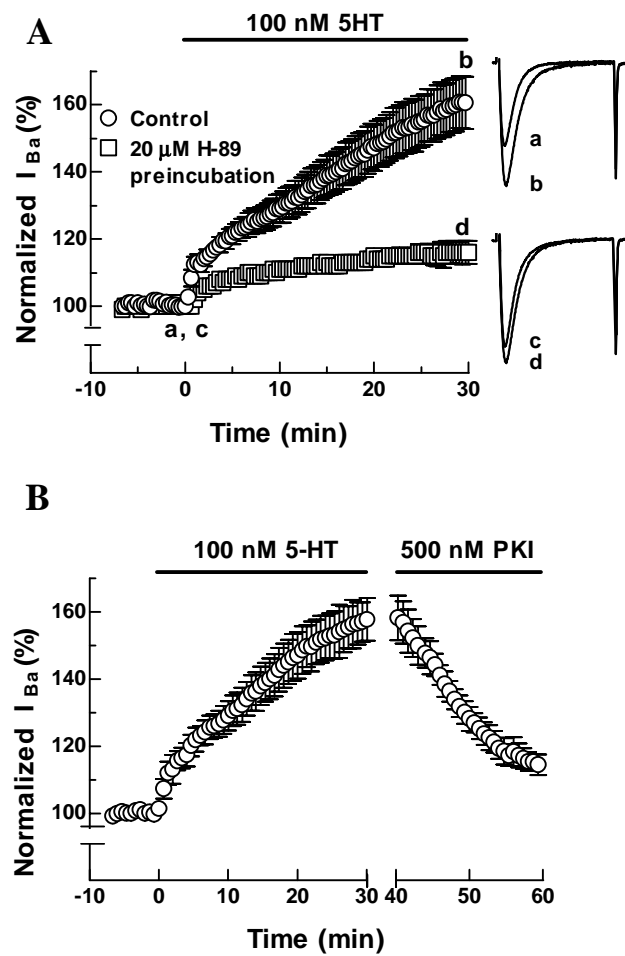


Figure 5

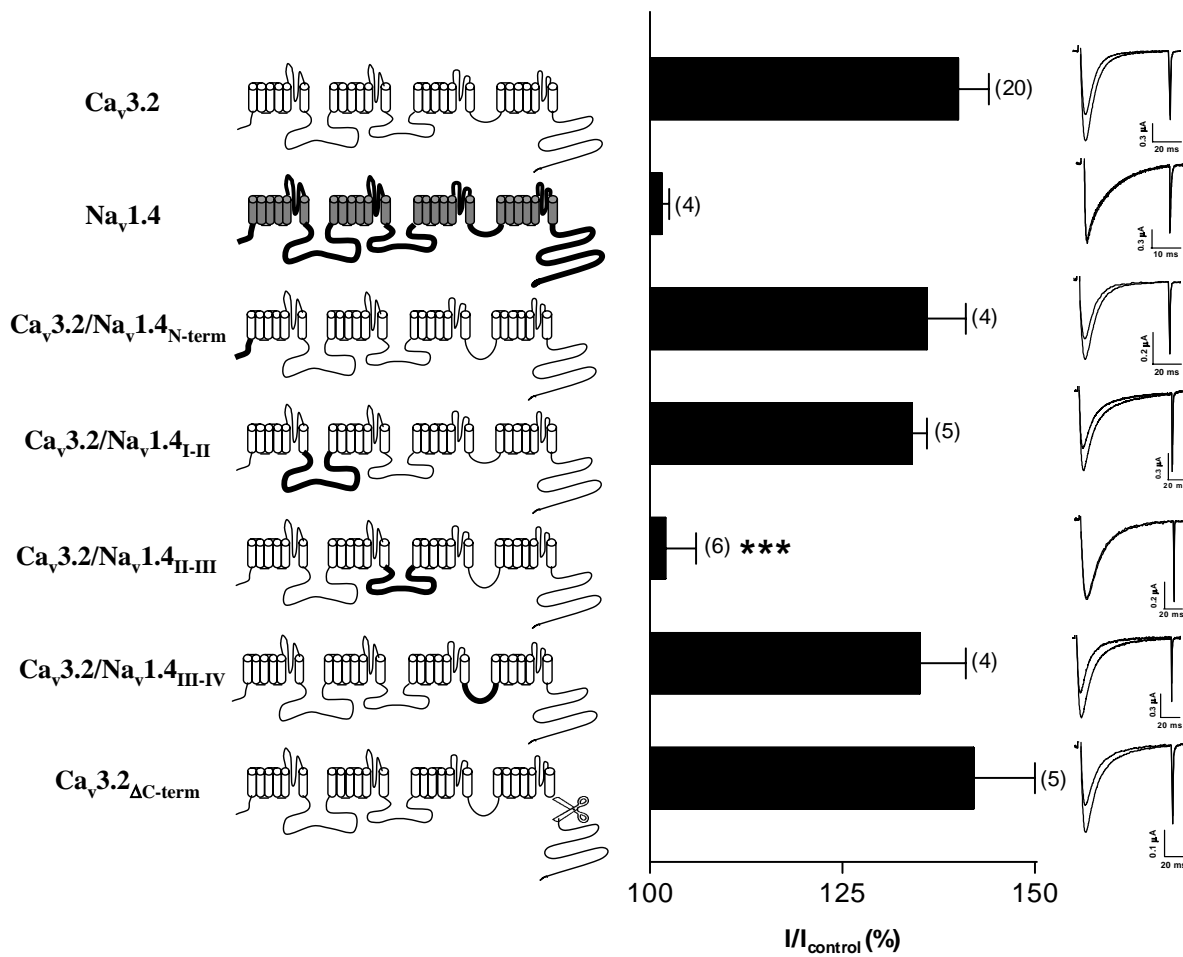


Figure 6